Not to appear in Nonlearned J., 45.

1 ## *Fermi* LAT Observation of Diffuse Gamma-Rays Produced Through
2 ## Interactions between Local Interstellar Matter and High Energy Cosmic Rays

3 A. A. Abdo[2,3], M. Ackermann[4], M. Ajello[4], W. B. Atwood[5], M. Axelsson[6,7], L. Baldini[8],

4 J. Ballet[9], G. Barbiellini[10,11], D. Bastieri[12,13], B. M. Baughman[14], K. Bechtol[4], R. Bellazzini[8],

5 B. Berenji[4], E. D. Bloom[4], E. Bonamente[15,16], A. W. Borgland[4], J. Bregeon[8], A. Brez[8],

6 M. Brigida[17,18], P. Bruel[19], T. H. Burnett[20], G. A. Caliandro[17,18], R. A. Cameron[4],

7 P. A. Caraveo[21], P. Carlson[22,7], J. M. Casandjian[9], C. Cecchi[15,16], Ö. Çelik[23], A. Chekhtman[2,24],

8 C. C. Cheung[23], S. Ciprini[15,16], R. Claus[4], J. Cohen-Tanugi[25], J. Conrad[26,7,22,27], S. Cutini[28],

9 C. D. Dermer[2], A. de Angelis[29], F. de Palma[17,18], S. W. Digel[4], E. do Couto e Silva[4], P. S. Drell[4],

10 R. Dubois[4], D. Dumora[30,31], C. Farnier[25], C. Favuzzi[17,18], S. J. Fegan[19], W. B. Focke[4],

11 M. Frailis[29], Y. Fukazawa[32], S. Funk[4], P. Fusco[17,18], F. Gargano[18], D. Gasparrini[28],

12 N. Gehrels[23,33], S. Germani[15,16], B. Giebels[19], N. Giglietto[17,18], F. Giordano[17,18], T. Glanzman[4],

13 G. Godfrey[4], I. A. Grenier[9], M.-H. Grondin[30,31], J. E. Grove[2], L. Guillemot[30,31], S. Guiriec[25,34],

14 Y. Hanabata[32], A. K. Harding[23], M. Hayashida[4], E. Hays[23], R. E. Hughes[14], G. Jóhannesson[4],

15 A. S. Johnson[4], R. P. Johnson[5], W. N. Johnson[2], T. Kamae[4], H. Katagiri[32], N. Kawai[35,36],

16 M. Kerr[20], J. Knödlseder[37], M. L. Kocian[4], F. Kuehn[14], M. Kuss[8], J. Lande[4], L. Latronico[8],

17 M. Lemoine-Goumard[30,31], F. Longo[38,10,11], F. Loparco[17,18], B. Lott[30,31], M. N. Lovellette[2],

18 P. Lubrano[15,16], A. Makeev[2,24], M. N. Mazziotta[18], J. E. McEnery[23], C. Meurer[26,7],

19 P. F. Michelson[4], W. Mitthumsiri[4], T. Mizuno[32,1], A. A. Moiseev[39,33], C. Monte[17,18],

20 M. E. Monzani[4], A. Morselli[40], I. V. Moskalenko[4], S. Murgia[4], P. L. Nolan[4], J. P. Norris[41],

21 E. Nuss[25], T. Ohsugi[32], A. Okumura[42], N. Omodei[8], E. Orlando[43], J. F. Ormes[41], M. Ozaki[44],

22 D. Paneque[4], J. H. Panetta[4], D. Parent[30,31], M. Pepe[15,16], M. Pesce-Rollins[8], F. Piron[25],

23 M. Pohl[45], T. A. Porter[5], S. Rainò[17,18], R. Rando[12,13], M. Razzano[8], A. Reimer[46,4],

24 O. Reimer[46,4], T. Reposeur[30,31], S. Ritz[23], L. S. Rochester[4], A. Y. Rodriguez[47], F. Ryde[22,7],

25 H. F.-W. Sadrozinski[5], D. Sanchez[19], A. Sander[14], P. M. Saz Parkinson[5], T. L. Schalk[5],

26 A. Sellerholm[26,7], C. Sgrò[8], D. A. Smith[30,31], P. D. Smith[14], G. Spandre[8], P. Spinelli[17,18],

27 J.-L. Starck[9], F. W. Stecker[23], M. S. Strickman[2], A. W. Strong[43], D. J. Suson[48], H. Tajima[4],

28 H. Takahashi[32], T. Takahashi[44], T. Tanaka[4], J. B. Thayer[4], J. G. Thayer[4], D. J. Thompson[23],

29 L. Tibaldo[12,13], D. F. Torres[49,47], G. Tosti[15,16], A. Tramacere[4,50], Y. Uchiyama[44,4], T. L. Usher[4],

30 V. Vasileiou[23,39,51], N. Vilchez[37], V. Vitale[40,52], A. P. Waite[4], P. Wang[4], B. L. Winer[14],

31 K. S. Wood[2], T. Ylinen[22,53,7], M. Ziegler[5]

[1] Corresponding author: T. Mizuno, mizuno@hep01.hepl.hiroshima-u.ac.jp.

[2] Space Science Division, Naval Research Laboratory, Washington, DC 20375, USA

[3] National Research Council Research Associate, National Academy of Sciences, Washington, DC 20001, USA

[4] W. W. Hansen Experimental Physics Laboratory, Kavli Institute for Particle Astrophysics and Cosmology, Department of Physics and SLAC National Accelerator Laboratory, Stanford University, Stanford, CA 94305, USA

[5] Santa Cruz Institute for Particle Physics, Department of Physics and Department of Astronomy and Astrophysics, University of California at Santa Cruz, Santa Cruz, CA 95064, USA

[6] Department of Astronomy, Stockholm University, SE-106 91 Stockholm, Sweden

[7] The Oskar Klein Centre for Cosmo Particle Physics, AlbaNova, SE-106 91 Stockholm, Sweden

[8] Istituto Nazionale di Fisica Nucleare, Sezione di Pisa, I-56127 Pisa, Italy

[9] Laboratoire AIM, CEA-IRFU/CNRS/Université Paris Diderot, Service d'Astrophysique, CEA Saclay, 91191 Gif sur Yvette, France

[10] Istituto Nazionale di Fisica Nucleare, Sezione di Trieste, I-34127 Trieste, Italy

[11] Dipartimento di Fisica, Università di Trieste, I-34127 Trieste, Italy

[12] Istituto Nazionale di Fisica Nucleare, Sezione di Padova, I-35131 Padova, Italy

[13] Dipartimento di Fisica "G. Galilei", Università di Padova, I-35131 Padova, Italy

[14] Department of Physics, Center for Cosmology and Astro-Particle Physics, The Ohio State University, Columbus, OH 43210, USA

[15] Istituto Nazionale di Fisica Nucleare, Sezione di Perugia, I-06123 Perugia, Italy

[16] Dipartimento di Fisica, Università degli Studi di Perugia, I-06123 Perugia, Italy

[17] Dipartimento di Fisica "M. Merlin" dell'Università e del Politecnico di Bari, I-70126 Bari, Italy

[18] Istituto Nazionale di Fisica Nucleare, Sezione di Bari, 70126 Bari, Italy

[19] Laboratoire Leprince-Ringuet, École polytechnique, CNRS/IN2P3, Palaiseau, France

[20] Department of Physics, University of Washington, Seattle, WA 98195-1560, USA

[21] INAF-Istituto di Astrofisica Spaziale e Fisica Cosmica, I-20133 Milano, Italy

[22] Department of Physics, Royal Institute of Technology (KTH), AlbaNova, SE-106 91 Stockholm, Sweden

[23] NASA Goddard Space Flight Center, Greenbelt, MD 20771, USA

[24] George Mason University, Fairfax, VA 22030, USA

[25] Laboratoire de Physique Théorique et Astroparticules, Université Montpellier 2, CNRS/IN2P3, Montpellier, France

[26] Department of Physics, Stockholm University, AlbaNova, SE-106 91 Stockholm, Sweden

[27] Royal Swedish Academy of Sciences Research Fellow, funded by a grant from the K. A. Wallenberg Foundation

[28] Agenzia Spaziale Italiana (ASI) Science Data Center, I-00044 Frascati (Roma), Italy

[29] Dipartimento di Fisica, Università di Udine and Istituto Nazionale di Fisica Nucleare, Sezione di Trieste, Gruppo

- 3 –

ABSTRACT

Observations by the Large Area Telescope (LAT) on the *Fermi* mission of diffuse γ-rays in a mid-latitude region in the third quadrant (Galactic longitude l from $200°$ to $260°$ and latitude $|b|$ from $22°$ to $60°$) are reported. The region contains no known large molecular cloud and most of the atomic hydrogen is within 1 kpc of the solar system. The contributions of γ-ray point sources and inverse Compton scattering are

Collegato di Udine, I-33100 Udine, Italy

[30]Université de Bordeaux, Centre d'Études Nucléaires Bordeaux Gradignan, UMR 5797, Gradignan, 33175, France

[31]CNRS/IN2P3, Centre d'Études Nucléaires Bordeaux Gradignan, UMR 5797, Gradignan, 33175, France

[32]Department of Physical Sciences, Hiroshima University, Higashi-Hiroshima, Hiroshima 739-8526, Japan

[33]University of Maryland, College Park, MD 20742, USA

[34]University of Alabama in Huntsville, Huntsville, AL 35899, USA

[35]Department of Physics, Tokyo Institute of Technology, Meguro City, Tokyo 152-8551, Japan

[36]Cosmic Radiation Laboratory, Institute of Physical and Chemical Research (RIKEN), Wako, Saitama 351-0198, Japan

[37]Centre d'Étude Spatiale des Rayonnements, CNRS/UPS, BP 44346, F-30128 Toulouse Cedex 4, France

[38]Istituto Nazionale di Fisica Nucleare, Sezione di Trieste, and Università di Trieste, I-34127 Trieste, Italy

[39]Center for Research and Exploration in Space Science and Technology (CRESST), NASA Goddard Space Flight Center, Greenbelt, MD 20771, USA

[40]Istituto Nazionale di Fisica Nucleare, Sezione di Roma "Tor Vergata", I-00133 Roma, Italy

[41]Department of Physics and Astronomy, University of Denver, Denver, CO 80208, USA

[42]Department of Physics, Graduate School of Science, University of Tokyo, 7-3-1 Hongo, Bunkyo-ku, Tokyo 113-0033, Japan

[43]Max-Planck Institut für extraterrestrische Physik, 85748 Garching, Germany

[44]Institute of Space and Astronautical Science, JAXA, 3-1-1 Yoshinodai, Sagamihara, Kanagawa 229-8510, Japan

[45]Department of Physics and Astronomy, Iowa State University, Ames, IA 50011-3160, USA

[46]Institut für Astro- und Teilchenphysik, Leopold-Franzens-Universität Innsbruck, A-6020 Innsbruck, Austria

[47]Institut de Ciencies de l'Espai (IEEC-CSIC), Campus UAB, 08193 Barcelona, Spain

[48]Department of Chemistry and Physics, Purdue University Calumet, Hammond, IN 46323-2094, USA

[49]Institució Catalana de Recerca i Estudis Avançats, Barcelona, Spain

[50]Consorzio Interuniversitario per la Fisica Spaziale (CIFS), I-10133 Torino, Italy

[51]University of Maryland, Baltimore County, Baltimore, MD 21250, USA

[52]Dipartimento di Fisica, Università di Roma "Tor Vergata", I-00133 Roma, Italy

[53]School of Pure and Applied Natural Sciences, University of Kalmar, SE-391 82 Kalmar, Sweden

estimated and subtracted. The residual γ-ray intensity exhibits a linear correlation with the atomic gas column density in energy from 100 MeV to 10 GeV. The measured integrated γ-ray emissivity is $(1.63 \pm 0.05) \times 10^{-26}$ photons s^{-1} sr^{-1} H-atom^{-1} and $(0.66 \pm 0.02) \times 10^{-26}$ photons s^{-1} sr^{-1} H-atom^{-1} above 100 MeV and above 300 MeV, respectively, with additional systematic error of ~ 10 %. The differential emissivity from 100 MeV to 10 GeV agrees with calculations based on cosmic ray spectra consistent with those directly measured, at the 10 % level. The results obtained indicate that cosmic ray nuclei spectra within 1 kpc from the solar system in regions studied are close to the local interstellar spectra inferred from direct measurements at the Earth within ~ 10 %.

Subject headings: cosmic rays – diffuse radiation – gamma rays: observations

1. Introduction

The diffuse high energy γ-ray emission ($E \geq 30$ MeV) has been interpreted to be a superposition of γ-rays produced via interactions between cosmic rays (CRs) and interstellar matter, inverse Compton (IC) scattering of interstellar soft photons off CR electrons, and the extragalactic diffuse γ-ray emission. The first component, if distinguished from the others, will enable using high-energy γ-ray observations for the study of the distribution of CRs and the interstellar medium. The distribution of neutral atomic hydrogen (H I) is traced by 21 cm line surveys and the molecular hydrogen distribution is derived indirectly using 2.6 mm line observations of carbon monoxide (CO). The total gas column density can also be traced indirectly from extinction and reddening by dust. Thus the spectrum and the flux of CRs can be obtained from sufficiently sensitive observations of high energy γ-rays. The observation of diffuse γ-rays away from the Galactic plane (Galactic latitude $|b| \geq 10°$) is suitable for studying local CRs, since diffuse γ-rays in such regions are less affected by contamination from strong point sources, and most of the gas along the line of sight is local. The SAS-2 (e.g., Fichtel, Simpson, & Thompson 1978) and COS-B observations (e.g., Lebrun et al. 1982) indicated a correlation between the γ-ray intensities and the total gas column densities at medium Galactic latitudes. Sreekumar et al. (1998) and Strong, Moskalenko, & Reimer (2004) showed a good correlation between the γ-ray intensities and model calculations in their analyses of the extragalactic diffuse emission observed by EGRET onboard the *Compton Gamma-Ray Observatory*. Despite these early studies, the flux and spectrum of local CRs deduced from γ-ray intensity remain uncertain, due to the possible contamination from unresolved point sources and uncertainties in modeling the IC contribution because of the large scale height of CR electrons and the reprocessing of the interstellar radiation by dust. Although CR nuclei in the vicinity of the solar system are thought to have spectral distributions and intensities similar to those measured at the Earth as reported by a number of γ-ray observations (e.g, Hunter et al. 1997; Digel et al. 2001), data above 1 GeV, which are crucial to distinguish CR nuclei spectra from that of CR electrons, have not been good enough due to the limited photon statistics and relatively limited energy coverage of these early missions.

The situation has improved significantly with the recent launch of the *Fermi* Gamma-ray Space Telescope on 2008 June 11. The *Fermi* LAT (Large Area Telescope) has a sensitivity that is more than an order of magnitude better than that of EGRET and enables resolving point sources and studying the diffuse γ-rays with unprecedented sensitivity. Recent advances of a CR propagation code GALPROP (e.g., Strong & Moskalenko 1998), which had been developed through comparisons with the EGRET data, allow us to predict and subtract IC emission and correlate γ-ray emission with interstellar matter more accurately.

In this paper, we present *Fermi* LAT observations of diffuse γ-rays in a mid-Galactic latitude region in the third quadrant (Galactic longitude l from 200° to 260° and $|b|$ from 22° to 60°). As discussed in the following sections, most of the gas along the line of sight is local, nearby on the scale of the Milky Way. The contribution from IC emission is only about 10 % of the total diffuse emission and the LAT has already resolved five times as many γ-ray point sources as previous missions in this region. These facts enable us to evaluate the local CR flux and the spectrum with small systematic uncertainty.

2. Observation and Data Reduction

The LAT is the main instrument of the *Fermi* Gamma-ray Space Telescope. It consists of 4×4 modules (towers) built with tungsten foils and silicon microstrip detectors to measure the arrival directions of incoming γ-rays, and a hodoscopic cesium iodide calorimeter to determine the photon energies. They are surrounded by 89 segmented plastic scintillators serving as an anticoincidence detector to reject charged particle events. Details of the LAT instrument and pre-launch expectations of the performance can be found in Atwood et al. (2009). The excellent sensitivity of the LAT is exemplified by initial publications such as Abdo et al. (2008).

Routine science operations with the LAT began on 2008 August 4. We have accumulated events from 2008 August 4 to 2009 January 31 to study diffuse γ-rays. During this time interval the LAT was operated in sky survey mode nearly all of the time; in this observing mode the LAT scans the sky, obtaining complete sky coverage every two orbits and relatively uniform exposures over time. We used the standard LAT analysis software, **ScienceTools** [1] version **v9r11**, and applied the following event selection criteria: (1) events have the highest probability of being photons, i.e., they are categorized as so-called diffuse class (Atwood et al. 2009), (2) the reconstructed zenith angles of the arrival direction of photons are selected to be less than 105°, in order to exclude periods where the Earth enters the LAT field of view, and (3) the center of the LAT field of view is within 39° from the zenith in order not to include the data taken in the pointed observation mode, because it has increased contamination from Earth albedo γ-rays. We also eliminated the period of time during which the LAT detected two bright GeV-emitting GRBs, i.e., GRB080916C

---

[1] available from the Fermi Science Support Center (`http://fermi.gsfc.nasa.gov/ssc/`)

(Abdo et al. 2009a) and GRB081024B (Omodei et al. 2008). We then generated count maps (using **gtbin** in **ScienceTools**) and exposure maps (using **gtexpcube**) in 13 logarithmically-sliced energy bins from 100 MeV to 9.05 GeV. A post-launch response function **P6_V3_DIFFUSE**, which was developed to account for the γ-ray detection inefficiencies that are correlated with trigger rate, was used in exposure calculations. These count and exposure maps were prepared in Cartesian coordinates in $0.5° \times 0.5°$ binning, and then transformed into HEALPix [2] (Górski et al. 2005) equal area sky maps of order=7. They are used below to correlate the γ-ray intensities with the column densities of atomic gas along the line of sight; the γ-ray intensity is calculated as the ratio of the counts and the exposures for each energy bin.

3. Data Analysis

3.1. Subtraction of Inverse Compton and Point Sources

To distinguish γ-rays produced in the interstellar medium from others, we referred to the GAL-PROP prediction of IC emission and an LAT source list for 6 month data [3]. This list was produced using a similar procedure used to obtain the LAT Bright Source List described by Abdo et al. (2009b). It covers the same period of time as that of our data set and contains 740 point sources with significance more than $5\,\sigma$. We adopted positions and spectral parameters from this list (single power-law model in 100 MeV–100 GeV) to estimate and subtract the photons from point sources to diffuse γ-ray emission. GALPROP (e.g., Strong & Moskalenko 1998) is a set of programs to solve the CR transport equation within our Galaxy and predict the γ-ray emission produced via inter-actions of CRs with interstellar matter (nucleon-nucleon interaction and electron bremsstrahlung) and soft photons (IC scattering). IC emission is calculated from the distribution of (propagated) electrons and the interstellar radiation fields developed by Moskalenko, Porter, & Strong (2006). Here we adopted the IC model map with version **54_5gXvarh7S** [4], which was used in another *Fermi* LAT paper to study the diffuse γ-ray emission in $10° \leq |b| \leq 20°$ (Abdo et al. 2009d). The CR electron spectrum is adjusted to agree with the directly-measured pre-Fermi spectrum in this GALPROP model. In order to minimize the uncertainty of the contribution from IC emission on the diffuse γ-ray spectrum, we selected sky regions away from the Galactic center; the lower CR electron fluxes and interstellar radiation field will result in dimmer IC emission than that toward the Galactic center. We chose the third quadrant, Galactic longitude l from $200°$ to $260°$ and the Galactic latitude b from $-60°$ to $-22°$ and from $22°$ to $60°$. The region is free of known large molecular clouds; Orion molecular clouds (Orion A and Orion B) and Monoceros molecular cloud complexes are located in the region l from $200°$ to $220°$ and b from $-10°$ to $-20°$, and the Tau-

---

[2] http://healpix.jpl.nasa.gov

[3] internally available to the LAT team

[4] The GALPROP galdef ID of this version is available at the website http://galprop.stanford.edu

128 rus/Perseus molecular clouds are in l from 150° to 185° (e.g., Dame, Hartmann, & Thaddeus 2001;
129 Digel et al. 1999; Digel & Grenier 2001). Therefore the region described is suitable for correlating
130 the γ-ray intensities with the local atomic-gas column densities.

131   In Figure 1, we show γ-ray count maps above 100 MeV. There are 52 sources in the LAT
132 6 month source list in our region of interest, more than five times as many sources in the third
133 EGRET catalog (Hartman et al. 1999) in this region (nine sources). The diffuse γ-ray spectrum,
134 after masking sources with circular regions of 1° radius, is shown in Figure 2. Atomic hydrogen
135 column density maps of the same region (see Section 3.2 for details) are given in Figure 3. In
136 Figure 2 and figures shown hereafter (Figures 4–6), the γ-ray intensities or CR fluxes multiplied by
137 E^2 (where E is the center of each energy bin in logarithmic scale) are presented. Also presented in
138 Figure 2 is the contribution from IC emission predicted by GALPROP, and the spillover from point
139 sources outside the mask regions estimated (using **gtmodel**) by the spectral parameters given in
140 the source list. Both the flux of estimated IC emission and the residual point source contribution are
141 less than 15 % of the total diffuse emission above 100 MeV. We thus conclude that the uncertainty
142 due to the IC and point source contributions is negligible after we subtract them from γ-ray data.
143 Hereafter we analyze diffuse emission after masking point sources and subtracting IC emission and
144 the residual contributions from point sources.

3.2.   Atomic Hydrogen Map

146   Column densities $N(\mathrm{H\,I})$ of atomic hydrogen gas were calculated from existing radio surveys
147 of the 21 cm line of H I. We used the Leiden/Argentine/Bonn (LAB) Survey which merges the
148 Leiden/Dwingeloo Survey (Hartmann & Burton 1997) with the Instituto Argentino de Radioas-
149 tronomia Survey (Arnal et al. 2000; Bajaja et al. 2005) and covers the entire sky. We applied an
150 optical depth correction under the assumption of a uniform spin temperature of 125 K and the cos-
151 mic microwave background intensity at 1420 MHz of 2.66 K (e.g., Hunter et al. 1994). The derived
152 H I column density maps of our region of interest are shown in Figure 3. Although major CO sur-
153 veys such as the one by Dame, Hartmann, & Thaddeus (2001) do not cover the region we analyzed,
154 no large molecular cloud is known there and the molecular gas contribution is expected to be small
155 due to the moderately high Galactic latitude. See the discussion by Dame, Hartmann, & Thaddeus
156 (2001) for the completeness of their survey. Hereafter we assume that all the gas is in atomic form
157 and traced by 21 cm radio surveys. Column densities of H I in our region range from 1×10^{20} cm^{-2}
158 up to 18×10^{20} cm^{-2} and the optical depth correction is rather small; the increase of the col-
159 umn densities from those for the optically thin case (infinite spin temperature) is ≤ 10 % in most
160 directions. On the assumption of a Galactic rotation curve by Clemens (1985) for the case of
161 $R_0 = 8.5$ kpc and $\theta_0 = 220$ km s^{-1} (where R_0 and θ_0 are the Galactocentric radius and the orbital
162 velocity of the local group of stars, respectively), we infer that, in almost every direction in our
163 region, more than 80 % of the H I along the line of sight is within 1 kpc of the solar circle. Further-
164 more, by referring to the vertical density distribution of H I given by Dickey & Lockman (1990),

we can conclude that more than 85 % of atomic gas in the line of sight is within 1 kpc of the solar system for $|b| \geq 22°$.

3.3. Correlation of γ-ray Intensities and Gas Column Densities

The LAT point-spread function (PSF) strongly depends on the photon energy (e.g., Atwood et al. 2009) and the energy dependence of the angular size needs to be taken into account in data analysis. We convolved the map of H I column densities obtained as described in Section 3.2 using the GaDGET package (Ackermann et al. 2008) with the LAT PSF for each of our energy bins; in the convolution we used the all sky map to take account of the contribution from outside the region for the analysis. Since the typical angular size of the variation of column densities is a few degrees (see Figure 3), only maps for the lowest energy bands (less than a few hundred MeV) are noticeably smeared.

The γ-ray intensities, after masking point sources with 1° circular regions and subtracting the IC emission and the residual point source contributions, are correlated with the H I column densities in each energy band. Both the γ-ray intensity map and the H I column density map were prepared in HEALPix equal area sky maps of order=7, whose pixel size in solid angle is 6.39×10^{-5} steradian and is close to that of 0.5×0.5 deg^2. We found a linear relationship between $N(\mathrm{H\,I})$ and residual γ-ray intensities for energies from 100 MeV to 10 GeV. Above 10 GeV the correlation is limited by photon statistics. Figure 4 shows the correlation between γ-ray intensities and the H I column densities for four representative energy bands. The linear correlation indicates that point source contributions are successfully subtracted and residual γ-rays mostly originate from interstellar atomic gas through interactions with CRs, plus isotropic diffuse component (extragalactic diffuse γ-rays, the residual particle background, and a possible residual of IC emission).

By fitting the correlation in each energy band with a linear function using a χ^2 minimization, we obtained the intensity of the isotropic diffuse component and the emissivity of atomic gas as the offset and the slope, respectively, as summarized in Table 1. Making the mask region larger, to 3° radius, gives consistent fit parameters within statistical errors, confirming that the contribution of point sources is well modeled and subtracted. The obtained isotropic diffuse component (offset column in Table 1) agrees within 10–20 % with the "Isotropic" component given in Abdo et al. (2009d) which investigates the medium-latitude diffuse emission. We note that the isotropic diffuse components obtained here and in Abdo et al. (2009d) include the residual background and thus should be regarded as an upper limit of the true extragalactic diffuse γ-ray emission. We also note that the adopted IC model affects the spectral shape and the intensity of our isotropic component, whereas it does not affect the emissivity significantly; modifying the IC emission by ± 50 % changes the offsets by 6 %–7 %, but alters the slopes less than 3 % except the lowest two energy bands. A detailed study of the extragalactic diffuse emission and the residual background using data for a larger sky area is underway and will be published elsewhere (A. A. Abdo et al. 2009, in preparation).

So far, we have been neglecting the contribution from CR interactions with ionized hydrogen (H II). The low-density ionized gas is unobservable, but can be inferred from dispersion measures of pulsar signals in the radio band. According to the model of Cordes & Lazio (2002), in the region we are studying, $N(\text{H II})$ is only $(1\text{–}2) \times 10^{20}$ cm^{-2} and fairly smooth. We thus conclude that the contribution from ionized gas does not affect the obtained emissivity significantly.

4. Discussion

With the approach described in Section 3, we succeeded in decoupling diffuse γ-rays related to the local atomic gas from point sources, the IC emission, and the isotropic diffuse component. The derived differential γ-ray emissivity from the local atomic gas is given in Figure 5. The systematic uncertainty of the effective area of the response we used (**P6_V3_DIFFUSE**) is estimated to be 10 %, 5 % and 20 % at 100 MeV, 560 MeV, and 10 GeV, respectively, and depend on the energy linearly in a logarithmic scale. This systematic uncertainty is comparable with the statistical error, and is indicated by the shaded area in the figure. The integral emissivity above 100 MeV and 300 MeV is $(1.63 \pm 0.05) \times 10^{-26}$ photons s^{-1} sr^{-1} H-atom^{-1} and $(0.66 \pm 0.02) \times 10^{-26}$ photons s^{-1} sr^{-1} H-atom^{-1}, respectively, with an additional systematic uncertainty of $\sim$ 10 %. These values can be compared with those reported by early measurements. SAS-2 (Fichtel, Simpson, & Thompson 1978) obtained about 3×10^{-26} photons s^{-1} sr^{-1} H-atom^{-1} and COS-B (Lebrun et al. 1982) reported $(1.67 \pm 0.24) \times 10^{-26}$ photons s^{-1} sr^{-1} H-atom^{-1} above 100 MeV. The EGRET analysis of various directions toward large molecular clouds (Digel et al. 2001) gives $(1.65\text{–}2.4) \times 10^{-26}$ photons s^{-1} sr^{-1} H-atom^{-1} and $(0.71\text{–}1.0) \times 10^{-26}$ photons s^{-1} sr^{-1} H-atom^{-1} above 100 MeV and 300 MeV, respectively. While most of these early measurements are consistent with the LAT data, the emissivity obtained by the LAT is much improved in photon statistics and energy range.

We can give constraints on the local CR spectrum by comparing the obtained emissivity with the model calculation of interactions between CRs and interstellar matter. Many evaluations of the γ-ray production due to CR interactions in the interstellar medium have been made, including Stecker (1973, 1989), Dermer (1986a,b), Bertsch et al. (1993), Mori (1997), Kamae et al. (2006) and Huang et al. (2007). In the calculation of neutral pion production and decay γ-rays, most authors have computed the γ-ray flux produced through interactions of high-energy CR protons with proton targets. The effects of heavy nuclei in both CRs and the target matter are usually taken into account as a so-called nuclear enhancement factor (ϵ_{M}) to multiply the proton-proton γ-ray yield. Although the predicted γ-ray spectra from proton-proton interactions assuming the same CR proton spectrum agree well ($\leq$ 10 %) among these works (e.g., Kamae et al. 2006), the nuclear enhancement factors differ by up to $\sim$ 30 %; the factors range from 1.45 to 1.80–2.0 as compiled by Mori (2009). Among them, Dermer (1986a,b) gives the lowest ϵ_{M} of 1.45, and Mori (2009) gives the highest ϵ_{M} of 1.84 at the CR proton kinetic energy of 10 GeV. His higher value of ϵ_{M} is attributed to the adoption of recent CR spectral formulae by Honda et al. (2004) and the

238 inclusion of nuclei heavier than He in both the interstellar medium and the CR spectra. We thus
239 regard ϵ_M by Mori (2009) as the most reliable.

240   In calculating the neutral pion production, we used the proton-proton interaction formalism by
241 Kamae et al. (2006). They gave parameterized formulae of the π^0 inclusive cross section and decay
242 γ-ray spectra for arbitrary proton kinetic energies from 0.488 GeV to 512 TeV. We adopted the
243 proton local interstellar spectrum (LIS) from the GALPROP model with **54_5gXvarh7S** and cal-
244 culated the γ-ray spectrum from nucleon-nucleon interactions using formulae given by Kamae et al.
245 (2006) under the assumption of the nuclear enhancement factor to be 1.84 as a representative value
246 of those by Mori (2009). In order to calculate the electron bremsstrahlung, we fully utilized GAL-
247 PROP which calculates the γ-ray spectrum using a formalism by Koch & Motz (1959) as explained
248 by Strong, Moskalenko, & Reimer (2000).

249   The predicted emissivity at the solar sytem (Galactocentric radius $R = 8.5$ kpc and the height
250 from the Galactic plane $z = 0$ kpc) is compared with our LAT measurement in Figure 5, and
251 the LIS of proton, electron and positron used in this model calculation is presented in Figure 6.
252 Also shown is a compilation of some measurements of proton and electron spectra at the Earth.
253 The proton and electron model spectra follow the observed ones above a few tens of GeV; below
254 this energy the solar wind lowers the observed fluxes. We note that the CR electron spectrum
255 measured by the LAT is somewhat harder than the GALPROP model (Abdo et al. 2009c), but
256 the effect on our analysis is negligible. We also note that the bremsstrahlung at around 100 MeV
257 has comparable contributions from both primary electrons and secondary electrons/positrons, as
258 discussed by Porter et al. (2008). Their contributions are included in the computed spectrum shown
259 in Figure 5.

260   The true LIS is somewhat uncertain due to solar activity. To model this solar modulation
261 effect on the CR spectrum, the formula by Gleeson & Axford (1968) generally has been used, in
262 which a single parameter ϕ is introduced. The proton LIS we adopted reproduces the observations
263 at the Earth with $\phi = 450$ MV as shown in Figure 6. The same data can also be reproduced by
264 a different formula of the LIS (dotted blue line) with $\phi = 600$ MV as described by Shikaze et al.
265 (2007). We thus regard the difference between two models as representing the uncertainty of the
266 LIS; they agree well (≤ 10 %) above 10 GeV and differ by ~ 20 % at about 3 GeV. This affects the
267 calculated emissivity by ~ 20 % and ≤ 10 % at about 100 MeV and above 1 GeV, respectively (e.g.,
268 Mori 1997). We note that the LIS we adopted better reproduces the observed proton spectrum
269 above 20 GeV. Although the true LIS below 1 GeV is highly uncertain, these CRs do not contribute
270 to the γ-ray emissivity above 100 MeV significantly.

271   As shown in Figure 5, the emissivity measured by the LAT agrees with the prediction from
272 the assumed LIS and the recent estimate of ϵ_M at the 10 % level, which is comparable with the
273 statistical error and the current systematic uncertainty of the LAT response. For reference, we
274 also show the γ-ray emissivity model obtained with the lowest ϵ_M (among references in Mori 2009)
275 of 1.45 that gives a predicted emissivity lower than that observed in 100 MeV–10 GeV. Since the

nucleon-nucleon component is dominant in the emissivity spectrum especially above 1 GeV, the observed agreement between the LAT data and the model calculation (with the latest estimate of ϵ_M) indicates that CR nuclei in the vicinity of the solar system in regions observed have spectral distributions and intensities close to those of the LIS inferred from measurements at the Earth within ~ 10 %. Although the constraint is rather weak, the agreement down to 100 MeV also suggests that highly uncertain low-energy (below a few hundred MeV) CR electron and positron spectra are compatible with our assumption (GALPROP model with **54_5gXvarh7S**) shown in Figure 6.

5. Summary and Conclusions

We report the observation of diffuse γ-rays in a mid-latitude region in the third quadrant using data from the first six months of *Fermi* LAT science observations. The region is away from the Galactic plane and the Galactic center, and contains no known large molecular cloud. Most of the atomic hydrogen is within 1 kpc of the solar system, and thus the region is suitable for studying the γ-ray emissivity of the local atomic gas and CR spectra in the neighborhood of the solar system. Thanks to the excellent performance of the LAT and recent developments of the CR propagation code and the interstellar radiation field model in GALPROP, we reliably estimated and subtracted the contribution from point sources and IC emission. The residual γ-ray intensities exhibit a linear relationship with the atomic gas column densities from 100 MeV to 10 GeV, indicating that non-isotropic γ-rays are produced through interactions of CRs with interstellar atomic gas. The measurement of the emissivity of local atomic hydrogen has already surpassed those by past missions in photon statistics and the energy range. It agrees with the prediction from CR spectra assumed, indicating that the CR nuclei spectra in the vicinity of the solar system in regions analyzed are close to the LIS inferred from direct measurements at the Earth within ~ 10 %. Low energy CR electron/positron spectra are suggested to be compatible with our assumption.

Some of the results in this paper have been derived using the HEALPix (Górski et al. 2005) package.

REFERENCES

Abdo, A. A. et al. 2008, Science, 322, 1218

Abdo, A. A. et al. 2009a, Science, 323, 1688

Abdo, A. A. et al. 2009b, ApJS, 183, 46

Abdo, A. A. et al. 2009c, Phys. Rev. Lett., 102, 181101

Abdo, A. A. et al. 2009d, Phys. Rev. Lett., submitted; see also Porter et al. (arXiv:0907.0294)

Ackermann, M., Jóhannesson, G., Digel, S., Moskalenko, I. V., Porter, A., Reimer, O., & Strong, A. 2008, in AIP Conf. Proc. 1085, High Energy Gamma-ray Astronomy, ed. F. A. Aharonian, W. Hofmann, & F. Rieger (New York: AIP), 763

Alcaraz, J. et al. 2000a, Phys. Lett. B., 472, 215

Alcaraz, J. et al. 2000b, Phys. Lett. B., 484, 10

Arnal, E. M., Bajaja, E., Larrarte, J. J., Morras, E., & Pöppel, W. G. L. 2000, A&AS, 142, 35

Atwood, W. B. et al. 2009, ApJ, 697, 1071

Bajaja, E., Arnal, E. M., Larrarte, J. J., Morras, R., Pöppel, W. G. L, & Kalberla, P. M. W. 2005, A&A, 440, 767

Barwick, S. W. et al. 1998, ApJ, 498, 779

Bertsch, D. L., Dame, T. M., Fichtel, C. E., Hunter, S. D., Sreekumar, P., Stacy, J. G., & Thaddeus, P. 1993, ApJ, 416, 587

Clemens, D. P. 1985, ApJ, 295, 422

Cordes, J. M., & Lazio, T. J. W. 2002, arXiv:astro-ph/0207156

Dame, T. M., Hartmann, D., & Thaddeus, P. 2001, ApJ, 547, 792

Dermer, C. D. 1986a, ApJ, 307, 47

Dermer, C. D. 1986b, A&A, 157, 223

Dickey, J. M., & Lockman, F. J. 1990, ARA&A, 28, 215

Digel, S. W., & Grenier, A. 2001, in AIP Conf. Proc. 587, Gamma-Ray Astrophysics, ed. S. Ritz, N. Gehrels, & C. R. Shrader (Melville, NY: AIP), 538

Digel, S. W., Aprile, E., Hunter, S. D., Mukherjee, R., Xu, F. 1999, ApJ, 520, 196

Digel, S. W., Grenier, I. A., Hunter, S. D., Dame, T. M., & Thaddeus, P. 2001, ApJ, 555, 12

Fichtel, C. E., Simpson, G. A., & Thompson, D. J. 1978, ApJ, 222, 833

Gleeson, N., & Axford, W. I. 1968, ApJ, 154, 1011

Górski, K. M., Hivon, E., Banday, A. J., Wandelt, B. D., Hansen, F. K., Reinecke, B., & Bartelmann, B. 2005, ApJ, 622, 759

Hartman, R. C. et al. 1999, ApJS, 123, 79

Hartmann, D., & Burton, W. B. 1997, Atlas of Galactic Neutral Hydrogen, (Cambridge, UK: Cambridge Univ. Press)

Honda, M., Kajita, T., Kasahara, K., & Midorikawa, S. 2004, Phys. Rev., D70, 043008

Huang, C. -Y., Park., S. -E., Pohl, M., & Daniels, C. D. 2007, Astroparticle Physics, 27, 429

Hunter, S. D., Digel, S. W., de Geus, E. J. & Kanbash, G. 1994, ApJ, 436, 216

Hunter, S. D. et al. 1997, ApJ, 481, 205

Kamae, T., Karlsson, N., Mizuno, T., Abe, T., & Koi, T. 2006, ApJ, 647, 692

Koch, H. W., & Motz, J. W. 1959, Rev. Mod. Phys., 31, 920

Lebrun, F. et al. 1982, A&A, 107, 390

Mori, M. 1997, ApJ, 478, 225

Mori, M. 2009, Astroparticle Physics, 31, 341

Moskalenko, I. V., Porter, T. A., & Strong, A. W., 2006, ApJ, 640, 155

Omodei, N. et al. 2008, GRB Coordinates Network, 8407

Porter, T., Moskalenko, I. V., Strong, A. W., Orlando, E., & Bouchet, L., 2008, ApJ, 682, 400

Sanuki, T. et al. 2000, ApJ, 545, 1135

Shikaze, Y. et al. 2007 Astroparticle Physics, 28, 154

Sreekumar, P. et al. 1998, ApJ, 494, 523

Stecker, F. W. 1973, ApJ, 185, 499

– 14 –

365 Stecker, F. W. 1989, in Cosmic Gamma Rays, Neutrinos and Related Astrophysics, ed. by M. M.
366   Shapiro and J. P. Wefel (Dordrecht; Kluwer), 85

367 Strong, A. W., & Moskalenko, I. V. 1998, ApJ, 509, 212

368 Strong, A. W., Moskalenko, I. V., & Reimber, O. 2000, ApJ, 537, 763

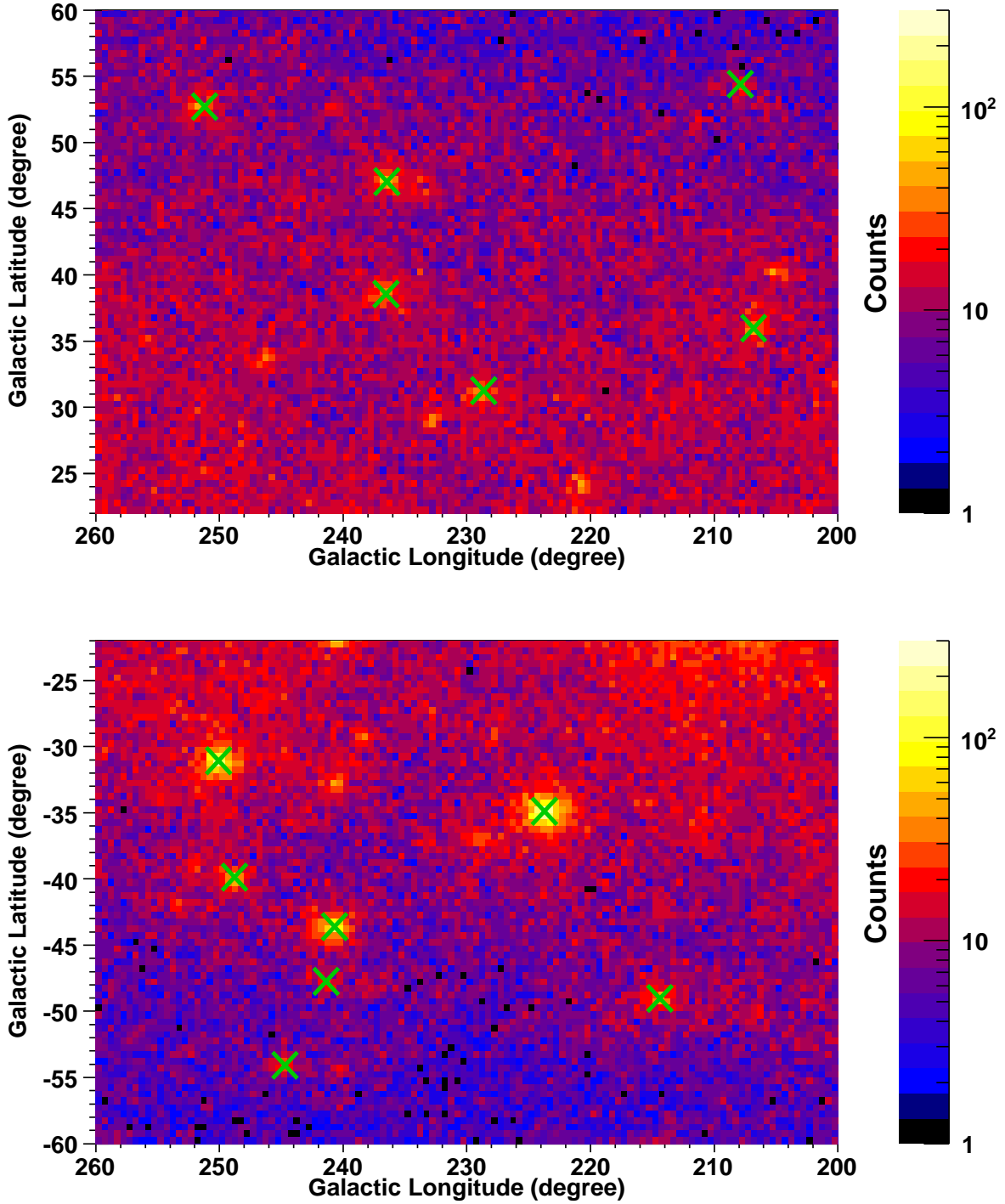369 Strong, A. W., Moskalenko, I. V., & Reimer, O. 2004, ApJ, 613, 956

Fig. 1.— *Fermi* LAT γ-ray count maps ($E \geq 100$ MeV) of regions we analyzed. Maps are in Cartesian projection with $0.5° \times 0.5°$ binning. The north and the south regions are shown in the upper panel and the lower panel, respectively. In these regions there are 52 sources in the LAT 6 month source list, of which 13 sources (indicated by green crosses) are included in the LAT Bright Source List (Abdo et al. 2009b).
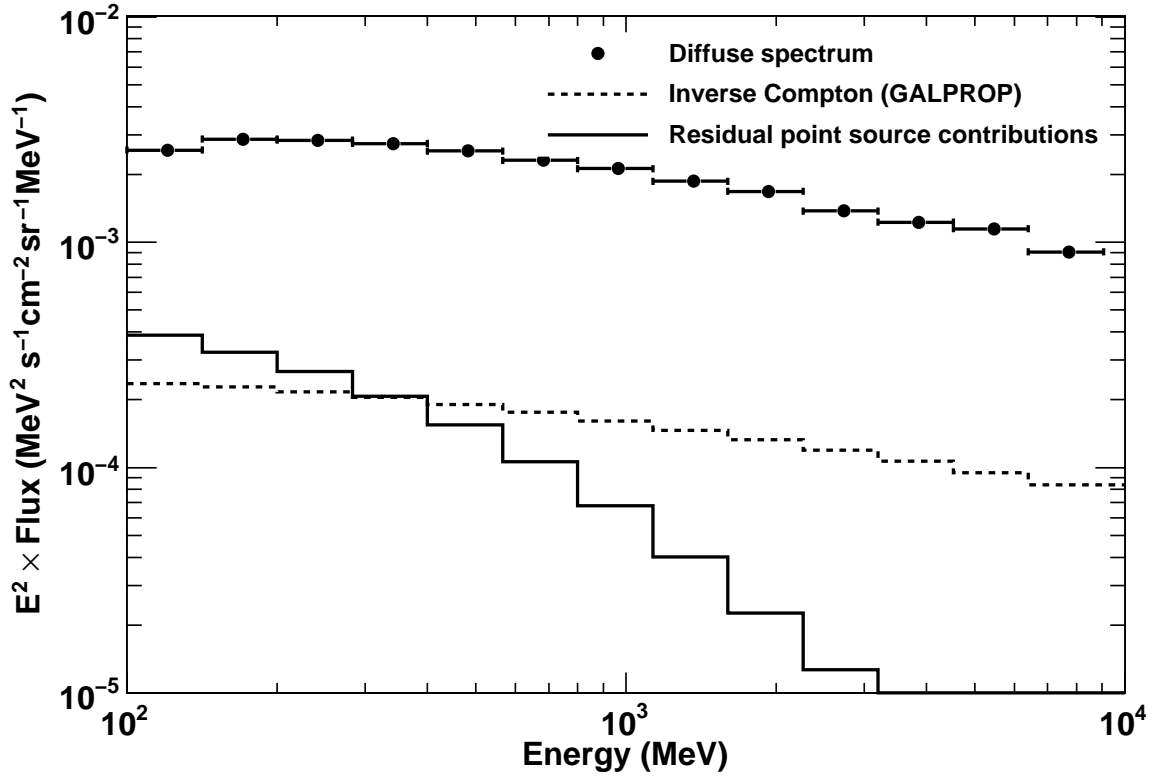
Fig. 2.— Diffuse γ-ray spectrum in regions analyzed (*l* from 200° to 260° and |*b*| from 22° to 60°) after masking point sources with circular regions of 1° radius. IC emission predicted by GALPROP (**54_5gXvarh7S**) and the residual point source contributions estimated from spectral parameters given in the LAT 6 month source list are shown by dotted and solid histograms, respectively. The horizontal and vertical error bars indicate the energy ranges and 1 σ statistical errors, respectively.
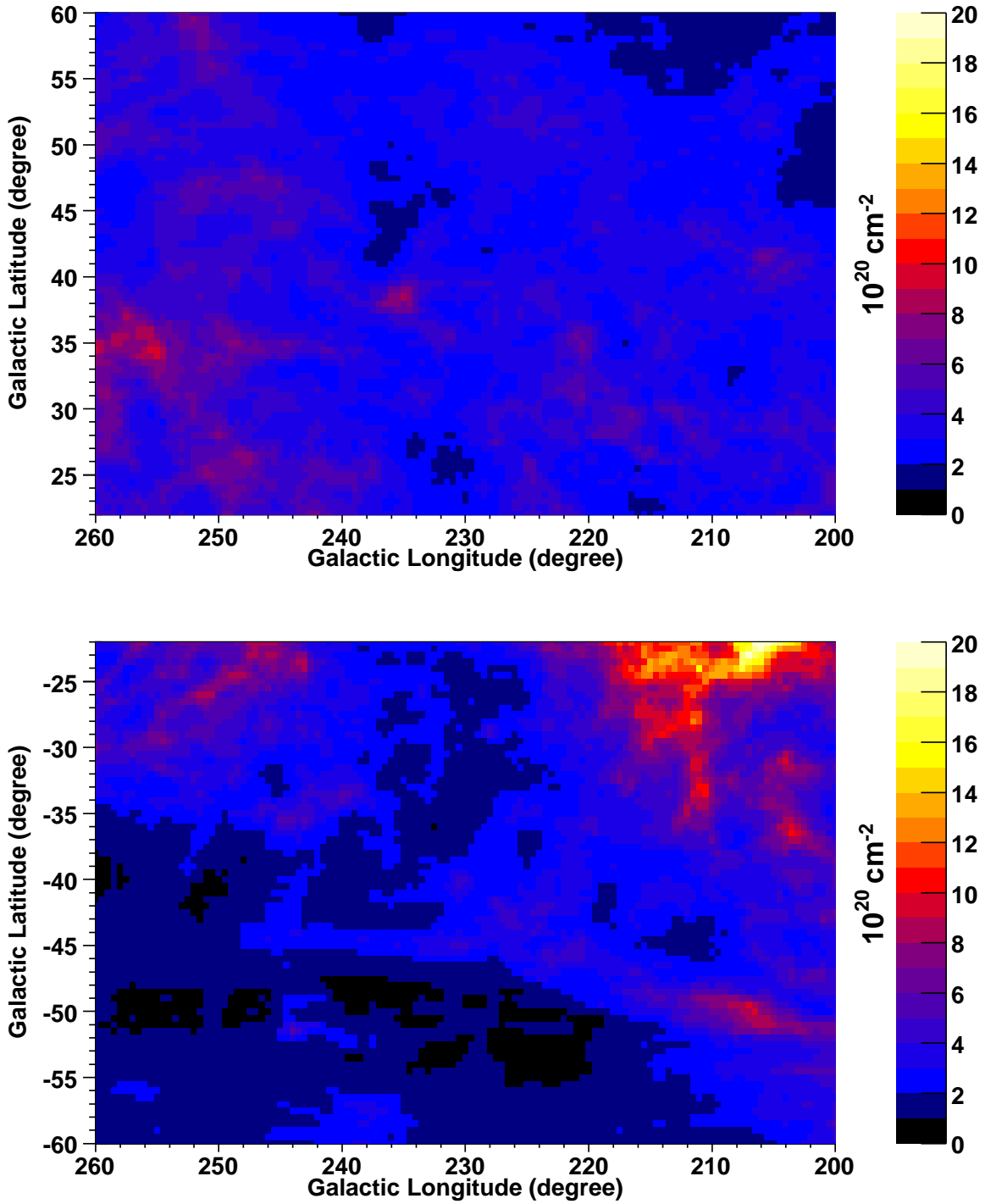
Fig. 3.— Column density maps of atomic hydrogen derived from the LAB survey under the assumption of a uniform spin temperature of 125 K.
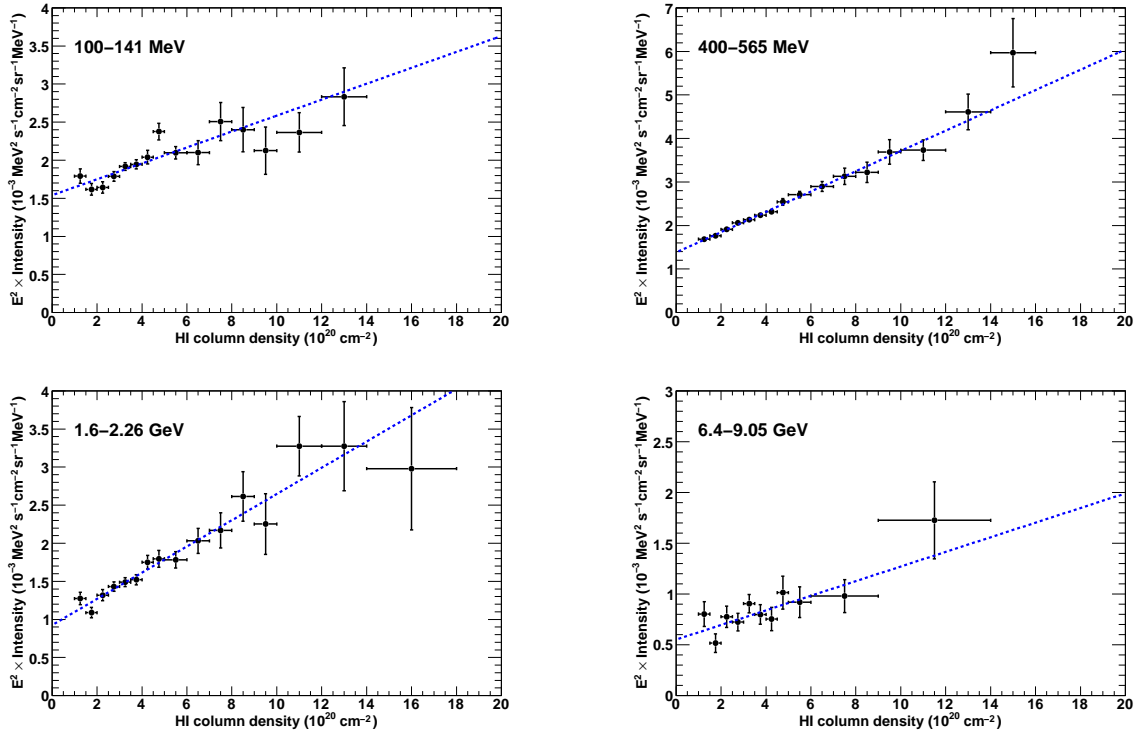
Fig. 4.— Correlation of the (IC and point-sources subtracted) γ-ray intensities and the H I column densities in four representative bands. The map of $N(\text{H I})$ (Figure 3) is convolved with the LAT PSF of the corresponding energy range. The horizontal and vertical error bars indicate the ranges of the column density and the $1\,\sigma$ statistical errors, respectively. Data in high energy range (above 1 GeV) are rebinned to have more than 10 γ-ray counts in each bin.
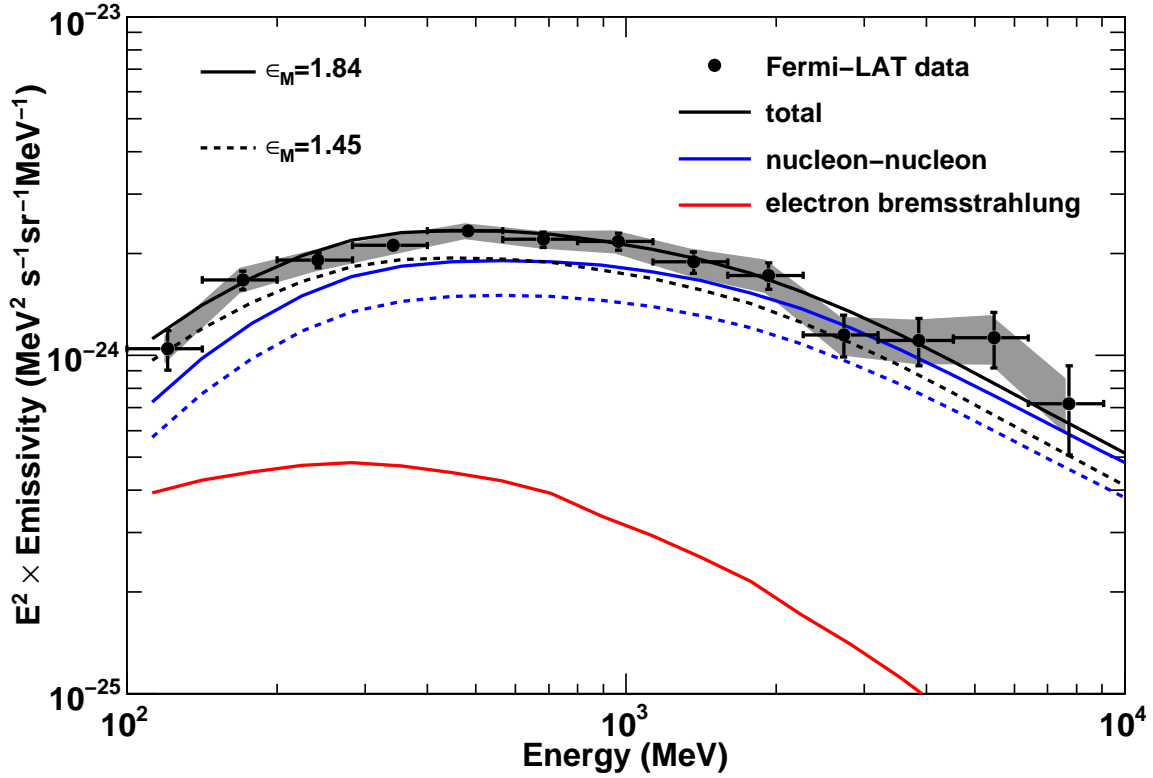
Fig. 5.— Differential γ-ray emissivity from the local atomic hydrogen gas compared with the calculated γ-ray production. The horizontal and vertical error bars indicate the energy ranges and 1 σ statistical errors, respectively. The assumed interstellar proton, electron and positron spectra are shown in Figure 6. Estimated systematic errors of the LAT data are indicated by the shaded area. A nucleus enhancement factor ϵ_{M} of 1.84 is assumed for the calculation of the γ-rays from nucleon-nucleon interactions. Dotted lines indicate the emissivities for the case of $\epsilon_{\mathrm{M}} = 1.45$, the lowest values in the referenced literature.
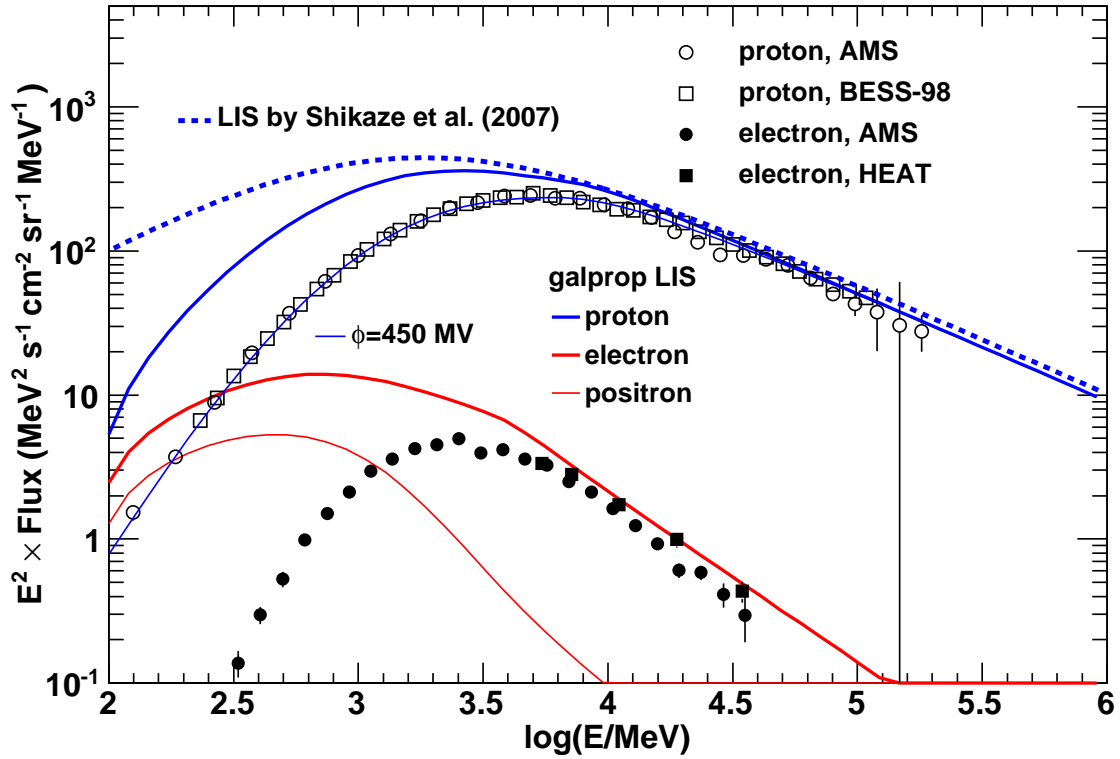
Fig. 6.— LIS of protons (thick blue line), electrons (thick red line) and positrons (thin red line) used to calculate the γ-ray emissivity model in Figure 5 with a compilation of direct measurements at the Earth; see Alcaraz et al. (2000a), Sanuki et al. (2000) and Shikaze et al. (2007) for proton data, and Alcaraz et al. (2000b) and Barwick et al. (1998) for electron data. Modulated spectrum with $\phi = 450$ MV is given by thin blue line. The proton LIS adopted by Shikaze et al. (2007) is shown by dotted blue line.

Table 1.   A summary of fit parameters with 1 Sigma statistical errors.

Energy GeV	Offset 10^{-4} MeV^2 s^{-1} cm^{-2} sr^{-1} MeV^{-1}	Slope 10^{-24} MeV^2 s^{-1} sr^{-1} MeV^{-1}	χ^2/dof [a]	Data/Model counts [b]
0.10–0.14	15.40 ± 0.54	1.04 ± 0.14	21.90/13	11799/11678
0.14–0.20	17.10 ± 0.40	1.67 ± 0.10	18.12/14	27891/27738
0.20–0.28	16.70 ± 0.36	1.91 ± 0.09	13.47/14	31718/31564
0.28–0.40	15.83 ± 0.36	2.11 ± 0.10	16.92/14	28987/28850
0.40–0.56	13.81 ± 0.39	2.33 ± 0.10	6.65/14	22718/22073
0.56–0.80	12.57 ± 0.41	2.20 ± 0.11	16.17/15	16137/16063
0.80–1.13	11.44 ± 0.44	2.17 ± 0.12	12.26/15	11421/11368
1.13–1.60	10.23 ± 0.49	1.88 ± 0.13	9.06/14	7364/7327
1.60–2.26	9.25 ± 0.54	1.72 ± 0.15	13.16/14	4765/4733
2.26–3.20	8.44 ± 0.58	1.15 ± 0.16	10.56/12	2764/2747
3.20–4.53	7.12 ± 0.64	1.10 ± 0.17	15.07/11	1733/1712
4.53–6.40	6.44 ± 0.75	1.12 ± 0.21	11.35/11	1158/1144
6.40–9.05	5.51 ± 0.77	0.71 ± 0.21	9.92/9	678/664

[a]Degree of freedom

[b]Data and model total counts after masking point sources with circular regions of $1°$ radius. We believe that the small (≤ 1 %) excesses of the data counts over the model counts are due to unresolved point sources or interstellar matter not traced by 21 cm line surveys.